Viscous flow and self-diffusion in densely and loosely packed metallic melts

S. Nell,[1,*] F. Yang,[1] Z. Evenson,[2] and A. Meyer[1]

[1]*Institut für Materialphysik im Weltraum, Deutsches Zentrum für Luft- und Raumfahrt (DLR), 51170 Köln, Germany*

[2]*Heinz Maier-Leibnitz Zentrum (MLZ) and Physik Department, Technische Universität München, 85748 Garching, Germany*

(Received 26 October 2020; revised 15 January 2021; accepted 19 January 2021; published 18 February 2021)

The Ni self-diffusion, density, and viscosity of the densely packed liquid $Ni_{66.7}B_{33.3}$ and the more loosely packed liquid $Ge_{66.7}Ni_{33.3}$ were measured with high accuracy using different experimental methods. The viscosity η was obtained using the oscillating-drop method combined with electrostatic levitation and the oscillating-cup technique in a rheometer. The Ni self-diffusion coefficient D_{Ni} was obtained from quasielastic neutron scattering experiments. For $Ni_{66.7}B_{33.3}$, it was found that the activation energies for self-diffusion and viscous flow, E_D and E_η, respectively, are almost equal. Hence, the product of the viscosity η and self-diffusion coefficient D is fairly constant over the entire temperature range measured, spanning almost 800 K. In contrast, for $Ge_{66.7}Ni_{33.3}$, $D\eta$ increases with increasing temperature, indicating that the dynamics in liquid $Ge_{66.7}Ni_{33.3}$ shows better agreement with an activated process. This temperature dependence is in line with the Stokes-Einstein relation.

DOI: 10.1103/PhysRevB.103.064206

I. INDRODUCTION

One question central to the topic of liquids is whether, and to what degree, the transport processes on macroscopic length scales can be understood and explained by microscopic processes. To answer this question, it is of fundamental importance to study and understand dynamical properties of liquids, such as self-diffusion and viscosity. In general, self-diffusion describes a single-particle diffusive transport. The viscosity, on the other hand, describes the macroscopic transport of momentum by the collective motion of different particles in a liquid. In liquids, the phenomenological Stokes-Einstein relation (SER) [1] is often used to determine the diffusion coefficient D of the liquid from its shear viscosity η:

$$D\eta = \frac{k_B T}{c\pi r_H}, \tag{1}$$

where r_H is the hydrodynamic radius, T is the temperature, and $k_B = 1.38 \times 10^{-23}$ J/K is the Boltzmann constant. c is a constant which has a value of 4 or 6 depending on slip or stick boundary conditions between the diffusing particle and the surrounding liquid [2]. If $c = 4$, Eq. (1) is called the Sutherland-Einstein relation (SuER) [3].

The SER is based on a rather simple model of one mesoscopic sphere immersed in a fluid with viscosity η but has been widely applied to derive D from η in liquids or vice versa [4–6]. This is particularly important where experimental difficulties occur (e.g., buoyancy-driven convection or chemical reactivity of the liquids with the crucible material), so that no reliable measurements for accurate diffusion or viscosity data exist. Here, the question is whether and under which conditions Eq. (1) still provides an applicable description of the relation between D and η if the size of the diffusing particle is generally on the order of that of the surrounding molecules/atoms of the medium. In organic liquids like benzol [7,8], tetramethylsilane [7,8], and methanol [9] and also in some metallic liquids [10,11] the SER was shown to be applicable within a factor of 2.

Many other studies [11–23], however, show that the SER deviates from the correlation observed between D and η. Its failure has often been attributed to so-called dynamical heterogeneity and is generally observed for deeply undercooled melts at low temperatures close to the glass transition temperature. In the case of dynamical heterogeneity, either the diffusion of the different components proceeds with different speeds [11], or there are different regions or domains in a liquid that exhibit different dynamics. For certain multicomponent metallic glass-forming melts, for instance, dynamical heterogeneity results in a melt viscosity that is dominated by the slowest-moving species [11], resulting in a fractional SER $D\eta \propto T^\alpha$.

Furthermore, there are also deviations from the SER at much higher temperatures, even far above the liquidus [12–16,23]. In $Zr_{64}Ni_{36}$ it has been experimentally observed over a broad temperature range spanning more than 800 K that $D\eta = \text{const}$ [12], in contrast to the SER, where $D\eta \propto T$. The observed deviation of liquid $Zr_{64}Ni_{36}$ from the SER cannot be explained by dynamical heterogeneity, as the diffusion coefficients of Zr and Ni were found to be equal within the experimental error [24]. This is, on the other hand, in line with the prediction of mode coupling theory (MCT) [25], where collective motions of diffusing particles are expected in densely packed melts [26]. Thus, the high atomic packing fraction of liquid $Zr_{64}Ni_{36}$ may be suggested as the reason for the violation of the SER, as the assumption of uncorrelated motion of the individual diffusing particles is no longer valid.

*Sarah.Nell@dlr.de

The onset of cooperative motion was also related recently to the deviation from Arrhenius-like melt dynamics in densely packed liquids at a characteristic temperature T_A [23,27–29] correlated strongly with the glass transition temperature T_g. This raises the question of whether the validity of the SER is generally related to the collectivity and the temperature dependence of the melt dynamics. Here, it appears that the packing fraction of the liquid is a key parameter. In order to investigate this in more depth, we performed accurate measurements of $Ni_{66.7}B_{33.3}$ and $Ge_{66.7}Ni_{33.3}$, which have considerably different packing fractions.

II. EXPERIMENTAL DETAILS

Packing fractions of $Ni_{66.7}B_{33.3}$ and $Ge_{66.7}Ni_{33.3}$ were calculated from the macroscopic density, which was measured with the containerless investigation technique of electrostatic levitation (ESL) [30,31]. The investigated sample was levitated in an electrostatic field under high vacuum ($< 10^{-7}$ mbar). Contactless heating and melting of the sample were achieved by two 25-W diode lasers (810 nm). The sample temperature was measured without contact by a single-color pyrometer with a wavelength of 1450 to 1800 nm, enabling temperature measurements between 300 °C and 2000 °C. Assuming that the emissivity is constant over the entire investigated temperature range, a correction of temperature was calculated from the liquidus temperature $T_{\mathrm{DSC,liq}}$, which was measured using a differential scanning experiment (DSC) with a heating/cooling rate of 10 K/min. We calculated the corrected temperature T_{corr} as follows: $T_{\mathrm{corr}} = (T_{\mathrm{pyro}}^{-1} + T_{\mathrm{DSC,liq}}^{-1} - T_{\mathrm{pyro,liq}}^{-1})^{-1}$. Here, T_{pyro} and $T_{\mathrm{pyro,liq}}$ are the sample temperature and the liquidus temperature observed on the pyrometer, respectively.

To determine the density, the levitated sample is illuminated from one side, and its shadow is recorded by a high-resolution camera with a frame rate of 250 Hz. An image-processing algorithm calculates the temperature-dependent sample volume from the edge curve of the sample profile under the assumption that, on average, the sample is symmetric with respect to its vertical axis. The duration of one density measurement was around 20 s. With knowledge of the sample mass (50 mg for $Ni_{66.7}B_{33.3}$ and 25 mg for $Ge_{66.7}Ni_{33.3}$), the temperature-dependent density could be determined with an overall uncertainty of $\frac{\Delta\rho}{\rho} < 1.7\%$.

Conventional techniques used for measuring the viscosity of liquids are container based, which are well suited to chemically inert liquids [30]. However, due to the high melting temperatures and the chemical reactivities of metallic melts, the measured data become unreliable when reactions occur between the melt and the container [30]. The nature and extent of the sample-container reaction depend on the temperature and the combination of the sample/crucible materials used for the measurement [32].

Containerless investigation techniques, such as levitation, circumvent this problem. ESL [30,31] in combination with the oscillating-drop method (ODM) [30,33] is one containerless technique used to measure the viscosity of levitated liquid droplets. With this method, accurate viscosity data can be obtained as long as a single oscillation mode dominates the viscous damping on an excited droplet [33]. Heintzmann *et al.* [33] showed for $Zr_{64}Ni_{36}$ that this is the case for data in the viscosity range of 10 to 250 mPa s using sample masses below 100 mg [33], where the measurement results show no dependence on the sample mass. In this work, the experimental setup for the viscosity measurements was the same as that used in the density measurements explained earlier. For measuring the viscosity of the levitated liquid sample, an additional sinusoidal voltage with a frequency between 185 and 255 Hz and an amplitude of 1 V to 3 kV was superimposed on the vertical levitation voltage, inducing an oscillation of the sample surface. After stopping the induced excitation, the sample oscillated freely, and the damping of its surface oscillation was recorded by a high-speed camera. The typical decay time is smaller than 0.5 s. Sample mass loss due to evaporation is negligible, as evidenced by weighing the sample mass before and after experimentation.

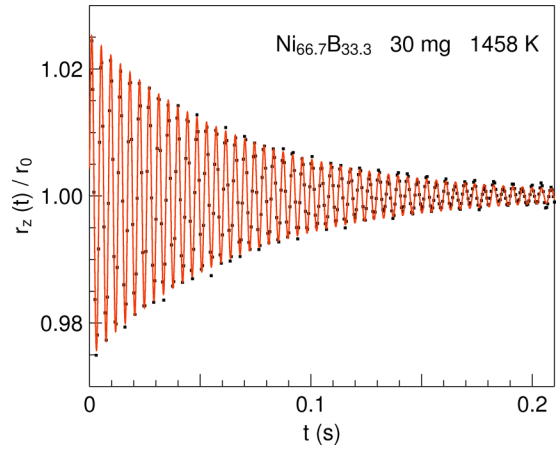

FIG. 1. Change in the vertical radius $r_z(t)$ normalized to the radius of the damped, spherical sample r_0 versus time t at 1458 K (black symbols). The red solid line is a fit of the data according to a damped sinus oscillation [12].

Figure 1 shows the damped oscillation of a $Ni_{66.7}B_{33.3}$ sample with a mass of 30 mg at 1458 K. Fitting the damped surface oscillation data provides the damping time τ, which is used to calculate the viscosity of the sample according to Lamb's law [34] as

$$\eta = \frac{\rho r_0^2}{5\tau}, \tag{2}$$

with ρ being the density of the sample and r_0 being the sample radius. Equation (2) is valid for the second oscillation mode. No additional modes were observed, which was verified by scrutinizing the Fourier transformed oscillation spectra, which showed just one single peak at the eigenfrequency of the sample. Thus, the damping of the liquid sample can be attributed solely to internal friction and hence the melt viscosity.

Additional measurements were carried out using the container-based oscillating-cup method (OCM) in a high-temperature oscillating-cup rheometer. OCM allows viscosity measurements of $Ni_{66.7}B_{33.3}$ in a higher temperature range without the deleterious effects resulting from evaporation of sample material occurring in ultrahigh-vacuum levitation experiments, which can lead not only to an instability of the levitating sample but also to non-negligible compositional

changes in the liquid alloy. The high-temperature oscillating-cup rheometer, which was used to measure the viscosity of $Ni_{66.7}B_{33.3}$ and $Ge_{66.7}Ni_{33.3}$, is described in detail elsewhere [35]. During the experiment, the investigated sample inside the cylindrical Al_2O_3 crucible ($Ø = 17$ mm) is placed in the center of a high-temperature vacuum furnace composed of graphite. The sample is heated under an argon atmosphere of $p = 400$ mbar. The sample temperature is measured by a pyrometer ($2.0 \leqslant \lambda \leqslant 2.7$ μm). The liquid sample is excited into torsional oscillation by an electrical motor. The damping, which is caused by the internal friction of the oscillating sample, is then determined by a position-sensitive detector, and the viscosity of the liquid sample is calculated by using the Roscoe equation [36,37]. The sample mass of the measured $Ni_{66.7}B_{33.3}$ sample was 55.0 g, and that of $Ge_{66.7}Ni_{33.3}$ was 27.6 g. Postmortem inspection of both samples showed no reaction with the Al_2O_3 crucible.

Quasielastic neutron scattering (QENS) probes the dynamics on atomic length and picosecond timescales, which results in accurate data, unaffected by convective flow. The Ni self-diffusion coefficients D_{Ni} on an absolute scale are obtained from the incoherent scattering of the Ni atoms present in the liquid samples [38,39]. To this end, QENS experiments were carried out at the neutron time-of-flight spectrometer TOFTOF [40] at the research neutron source Heinz Maier-Leibnitz (FRM II) of the Technische Universität München. To prepare the $Ni_{66.7}B_{33.3}$ sample for the QENS experiments, ^{nat}B was substituted with the stable isotope ^{11}B due to its significantly smaller neutron absorption cross section ($\sigma_{abs} = 0.0055$ barn [41]) compared to that of ^{nat}B ($\sigma_{abs} = 767.0$ barns [41]). The incident neutron wavelength of 7 Å provides an accessible range of momentum transfer q between 0.2 and 1.6 $Å^{-1}$ at zero energy transfer. In this q range, the signal is dominated by incoherent scattering of Ni for both investigated alloys. With a chopper speed of 6000 rpm the instrumental energy resolution result is $\simeq 70$ μeV at the full width at half maximum. Using the ESL device, the roughly spherical and electrically charged $Ni_{66.7}B_{33.3}$ sample with a mass of 470 mg was levitated and processed in a high-vacuum atmosphere ($< 10^{-7}$ mbar). Self-diffusion coefficients D_{Ni} were determined between 1264 and 1495 K for 60 min at each measurement temperature. Due to the containerless processing environment, heterogeneous nucleation resulting from sample-crucible contact was avoided, and undercoolings of up to 140 K were achieved.

Like for the viscosity measurement, to avoid a loss of sample stability in the ESL, D_{Ni} of $Ni_{66.7}B_{33.3}$ and $Ge_{66.7}Ni_{33.3}$ were obtained in the highest temperature range using a high-temperature Nb electrical resistance furnace (HTF). In these experiments, the sample was placed in a cylindrical 0.5-mm thin-walled Al_2O_3 container. The liquid $Ni_{66.7}B_{33.3}$ sample had a mass of 5 g, a diameter of 5 mm, and a height of about 30 mm. Measurements on $Ni_{66.7}B_{33.3}$ were performed at temperatures between 1413 and 1823 K for anywhere between 60 and 120 min at each temperature. The cylindrical $Ge_{66.7}Ni_{33.3}$ sample with a mass of 3.5 g, a diameter of 5 mm, and a height of roughly 30 mm was measured at temperatures between 1123 and 1393 K, with each measurement lasting 90 min. Both alloys showed no reaction with the crucible. To analyze the experimental data the FRIDA [42] software was used. The measured time-of-flight spectra were normalized to a vanadium standard and corrected for detector efficiency, self-absorption, and container scattering before final interpolation to constant wave numbers q. Figure 2 shows the resulting spectra of the dynamic structure factor $S(q, \omega)$ of liquid $Ni_{66.7}B_{33.3}$ at 1593 K. Solid lines are fits of a Lorentzian function convoluted with the energy resolution function.

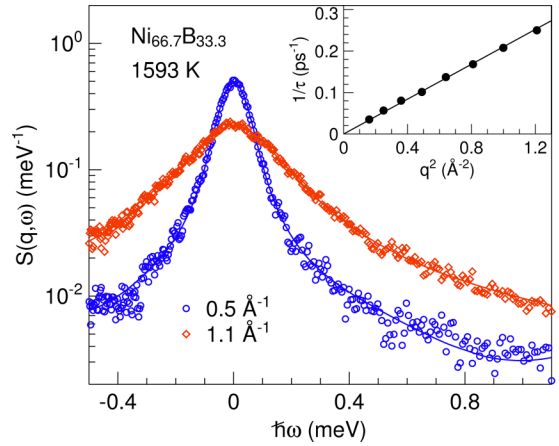

FIG. 2. Dynamic structure factor $S(q, \omega)$ of liquid $Ni_{66.7}B_{33.3}$ at 1593 K and q values of 0.5 and 1.1 $Å^{-1}$. Solid lines are fits with a Lorentzian function convoluted with the energy resolution function. Inset: Inverse relaxation time $1/\tau$ versus q^2. The diffusion coefficient is then derived according to the slope $D = 1/\tau q^2$.

III. RESULTS AND DISCUSSION

The top panel of Fig. 3 shows the density of $Ni_{66.7}B_{33.3}$ and $Ge_{66.7}Ni_{33.3}$ compared to the data of $Zr_{64}Ni_{36}$ [12].

Using the sample density ρ and the covalent radii r_i [43] of element i, the effective volume packing fraction ϕ was calculated using $\phi = (4\pi/3 \sum_i c_i r_i^3)/[(M/\rho)/N_A]$. Here, c_i represents the respective concentration of element i in the alloy. M is the molar mass of the alloy, and $N_A = 6.022 \times 10^{23}$ $mol^{-1}$is Avogadro's constant. The results are shown in the bottom panel of Fig. 3. $Ni_{66.7}B_{33.3}$ is similar to $Zr_{64}Ni_{36}$ (0.55 ± 0.002 at T_{liq} [12]), a dense-packed system with a packing fraction of 0.52 at its liquidus temperature $T_{liq} =$ 1398 K [44]. $Ge_{66.7}Ni_{33.3}$ has a lower packing fraction, which is in line with the microscopic structure of the melts [45,46]. At the liquidus temperature $T_{liq} = 1035$ K [44] the packing fraction of $Ge_{66.7}Ni_{33.3}$ $\phi = 0.43$ (see Fig. 3).

The top panel of Fig. 4 shows the temperature-dependent melt viscosity of $Ni_{66.7}B_{33.3}$, which increases with decreasing temperature. The viscosity of $Ni_{66.7}B_{33.3}$ was obtained in a temperature range of some 325 K, from ~1250 to ~1575 K, and a viscosity range of 8 to 30 mPa s using the ODM in combination with ESL. The results are shown in the top panel of Fig. 4 by red squares. Solid red squares show data obtained using a sample mass of 30 mg; open red squares represent data for a 50-mg sample. Measurements for two different sample masses were carried out in order to exclude possible systematic errors due to nonlinear droplet oscillations on the resulting viscosities [12,33,47]. In this work, no sample

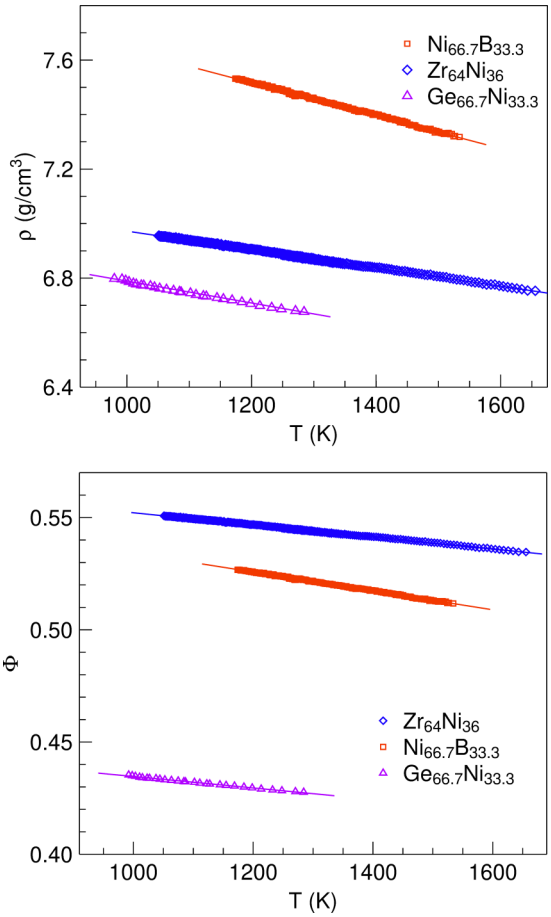

FIG. 3. Top: Density of $Ni_{66.7}B_{33.3}$ (red squares), $Ge_{66.7}Ni_{33.3}$ (purple triangles), and $Zr_{64}Ni_{36}$ [12] (blue diamonds) in dependency of temperature measured by using ESL. Bottom: Packing fraction of $Ni_{66.7}B_{33.3}$ (red squares), $Ge_{66.7}Ni_{33.3}$ (purple triangles), and $Zr_{64}Ni_{36}$ [12] (blue diamonds). The solid lines are linear fits.

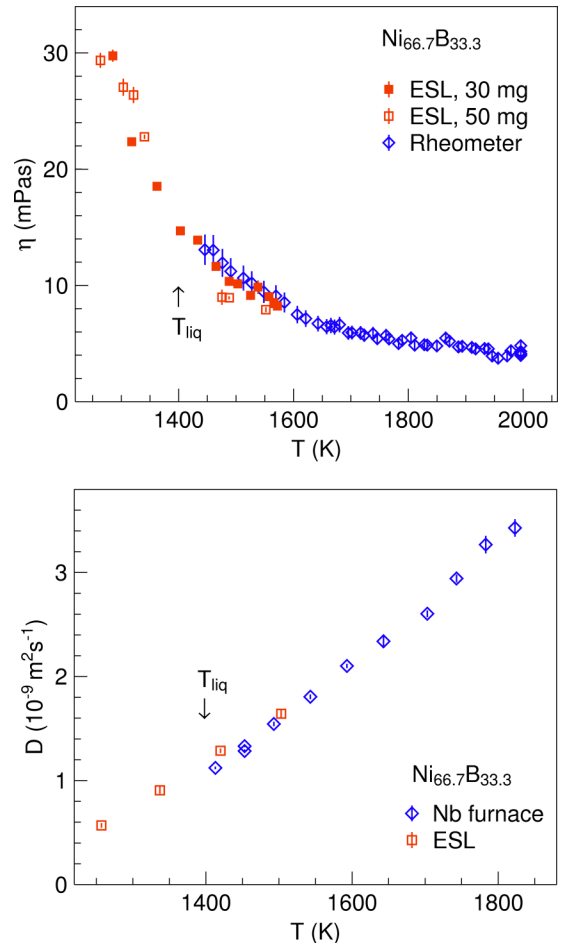

FIG. 4. Top: Viscosity of $Ni_{66.7}B_{33.3}$ versus temperature. Blue diamonds represent η measured with the OCM in the rheometer. The red squares correspond to data measured for different sample masses using the ODM in combination with ESL. Solid red squares show data obtained using a sample mass of 30 mg; open red squares represent data for a 50-mg sample. Bottom: Ni self-diffusion coefficient of $Ni_{66.7}B_{33.3}$ versus temperature. Red squares show data obtained using ESL; blue diamonds show data using the Nb electrical resistance furnace.

mass dependence of the derived viscosity (between 30 and 50 mg) via ODM combined with ESL (see Fig. 4, top panel) is found. Data obtained using the rheometer are shown in the top panel of Fig. 4 by blue diamonds. Here, the data cover a temperature range of some 550 K, from ∼1450 to ∼2000 K, and a viscosity range from 4 to 13 mPa s. The results obtained by the two methods agree within the measurement uncertainties. This supports the conclusion that during the rheometer experiment no reaction between the sample and crucible took place and further that we measured accurate data by using this method since we know that ESL delivers accurate viscosity data of the best quality. By combining the results of both methods (ESL and rheometer), it was possible to measure accurate viscosity data over a wide temperature range of more than 700 K. The temperature-dependent self-diffusion coefficients of $Ni_{66.7}B_{33.3}$ are depicted in the bottom panel of Fig. 4, showing the expected increase in D_{Ni} with increasing temperature. The results obtained using the two different sample environments, ESL and HTF, agree within the measurement uncertainties. By combining measurements in both sample environments, accurate self-diffusion coefficients D_{Ni} of $Ni_{66.7}B_{33.3}$ over a broad temperature range of some 500 K, between 1280 and 1780 K, were obtained.

Figure 5 displays the viscosity and diffusion data of $Ni_{66.7}B_{33.3}$ and $Ge_{66.7}Ni_{33.3}$, compared with those of $Zr_{64}Ni_{36}$ [12]. The viscosity of $Ge_{66.7}Ni_{33.3}$ is, in contrast to the viscosity of $Ni_{66.7}B_{33.3}$ and $Zr_{64}Ni_{36}$ [12], 4 times smaller at the same temperature, whereas $Ni_{66.7}B_{33.3}$ and $Zr_{64}Ni_{36}$ show similar viscosities at the same temperature. A similar qualitative trend is observed for the Ni self-diffusion coefficient (top panel), where the Ni self-diffusion coefficient of $Ge_{66.7}Ni_{33.3}$ is more than 3 times faster than that of $Ni_{66.7}B_{33.3}$ and $Zr_{64}Ni_{36}$ [12] at the same temperature.

Temperature-dependent dynamics over a large temperature range are known to deviate from Arrhenius-like behavior. This was already observed for $Zr_{64}Ni_{36}$ [12,31]. In Fig. 5, we fitted the data (blue diamonds) with the power law [48] of MCT (blue solid lines), which is

$$\eta(T) = \eta_0 \left(\frac{T - T_c}{T_c} \right)^{\gamma}. \tag{3}$$

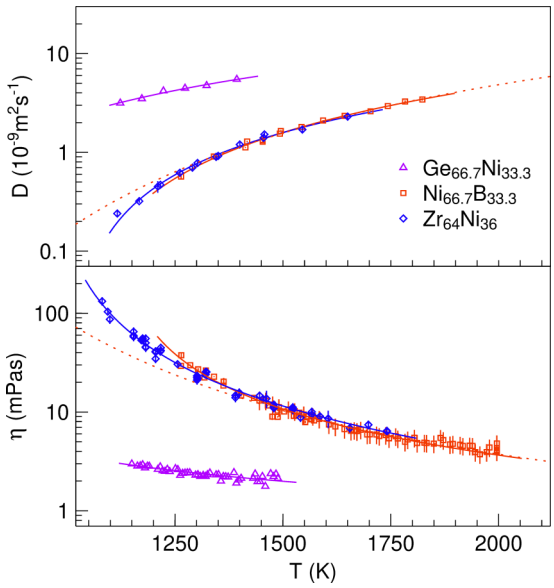

FIG. 5. Top: Ni self-diffusion coefficients of $Ni_{66.7}B_{33.3}$ (red squares) and $Ge_{66.7}Ni_{33.3}$ (purple triangles) as a function of temperature in comparison with the Ni self-diffusion coefficient of $Zr_{64}Ni_{36}$ (blue diamonds) [12]. Bottom: Viscosity of $Ni_{66.7}B_{33.3}$ (red squares), $Ge_{66.7}Ni_{33.3}$ (purple triangles), and $Zr_{64}Ni_{36}$ [12] (blue diamonds). The blue and red solid lines are corresponding fits of the power law; the purple solid line and the red dashed line are fits of Arrhenius's law.

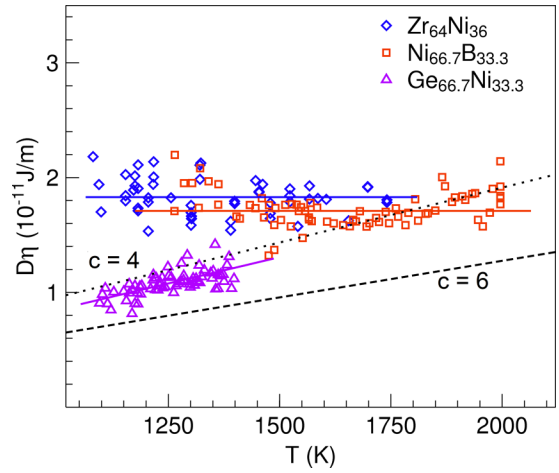

FIG. 6. $D_{Ni}\eta$ as a function of temperature. Red squares show the data for $Ni_{66.7}B_{33.3}$, and purple triangles show data for $Ge_{66.7}Ni_{33.3}$. In comparison $D_{Ni}\eta$ of $Zr_{64}Ni_{36}$ is shown by blue diamonds [12]. The SER is shown as a dashed line with different values of c [see Eq. (1)], where the covalent radius of Ni is chosen as the hydrodynamic radius $r_{Ni} = r_H = 1.15$ Å [43]. Solid lines are guides to the eye.

Here, η_0 describes a scaling factor, and T_c and γ are the critical temperature and the critical exponent of MCT, which are material-dependent parameters [25]. The red solid lines in Fig. 5 correspond to a power-law fit of the data of $Ni_{66.7}B_{33.3}$ (red squares). The resulting fit parameters are $\eta_0 = (2.8 \pm 0.1)$ mPa s, $T_c = (1094.3 \pm 26.9)$ K, and $\gamma = (-1.3 \pm 0.1)$, and for the Ni self-diffusion they are $D_0 = (4.6 \pm 1.1) \times 10^{-8}$ m^{2}s^{-1}, $T_c = (991.6 \pm 79.3)$ K, and $\gamma = (1.6 \pm 0.2)$. Red dashed lines correspond to an Arrhenius fit of the data for $Ni_{66.7}B_{33.3}$; purple solid lines correspond to an Arrhenius fit of the data for $Ge_{66.7}Ni_{33.3}$.

To check the relation between the viscosity and the Ni self-diffusion in the obtained alloys, the measured viscosity is multiplied by the fit of D_{Ni}. Figure 6 shows $D\eta$ as a function of temperature for $Ni_{66.7}B_{33.3}$ and $Ge_{66.7}Ni_{33.3}$, as well as for $Zr_{64}Ni_{36}$ for purposes of comparison [12].

The experimental data for $Ge_{66.7}Ni_{33.3}$ show a temperature-dependent behavior with the same trend as that predicted by the SER, with the measured data $D\eta$ increasing with increasing temperature (see Fig. 6). Due to the low atomic packing fraction of liquid $Ge_{66.7}Ni_{33.3}$, the assumption of uncorrelated motion of one individual diffusing particle is nearly fulfilled, which leads to the same temperature-dependent behavior as predicted by the SER.

For $Ni_{66.7}B_{33.3}$ the product is $(1.7 \pm 0.18) \times 10^{-11}$ J/m and constant over the entire measured temperature range, showing the same behavior as $Zr_{64}Ni_{36}$, with an absolute value in agreement within the standard measurement error [12]. For comparison, the SER is also shown in Fig. 6 as a dashed line with different values of c depending on slip ($c = 4$) or stick ($c = 6$) boundary conditions between the diffusing particle and the surrounding liquid [2] [see Eq. (1)]. The covalent radius of Ni is, in both cases ($c = 4$ or 6), chosen to be hydrodynamic radius $r_{Ni} = r_H = 1.15$ Å [43].

In the case of $Ni_{66.7}B_{33.3}$ and $Zr_{64}Ni_{36}$ [12] the experimental data are underestimated by more than a factor of 2 when compared to the SER if $c = 6$. Even by using the SuER ($c = 4$), the experimental data can be reproduced only in the region of ~1750 K. Above 1750 K the D values for $Ni_{66.7}B_{33.3}$ are extrapolated and hence subject to a major uncertainty. The absolute values of the experimental data cannot be reproduced over the entire measured temperature range of some 800 K, the temperature dependence of the experimental data, where $D\eta = \text{const}$, is significantly different from the SER/SuER model prediction ($D\eta \propto k_B T$; see Fig. 6). The value of the product $D\eta$ is better predicted, particularly near the liquidus temperature, if, e.g., the Goldschmidt radius (1.25 Å [44]) is used instead of the covalent radius. However, the deviation of the temperature-dependent $D\eta$ over the measured temperature range is even larger. Describing the experimental data with the SER/SuER is possible only when assuming a temperature-dependent hydrodynamic radius of Ni, instead of a static, covalent radius. In order to obtain an accurate description of the experimental data using the SER, this temperature-dependent radius would have to double in value in the investigated temperature range—a scenario that is physically unrealistic. The observation that $D\eta \approx \text{const}$, in agreement with the prediction of the MCT, has been attributed to a highly collective nature of the atomic motion in glass-forming liquids [12,15,26]. This appears to be the case for $Zr_{64}Ni_{36}$ and $Ni_{66.7}B_{33.3}$, even at temperatures well above the critical temperature of MCT, where a dominant structural relaxation timescale governs both the self-diffusion and the melt viscosity [49]. Furthermore, molecular dynamics simulations of Zr-Cu by Han and Schober [15] have demonstrated

that $D\eta \approx$ const up to a temperature of 200 K above the liquidus.

The onset of collective dynamics has been also associated with deviations of the experimental data from Arrhenius-like behavior at a temperature T_A [23,27–29]. For $Zr_{64}Ni_{36}$ and $Ni_{66.7}B_{33.3}$ in the studied temperature range, this occurs at 1300 K [31] and 1350 K (see Fig. 5, red dashed and solid lines), respectively. However, for both alloys, above and below this temperature, the relation $D\eta \approx$ const is observed. Taking this to be an indicator of highly correlated atomic motion, we find that collective dynamics is present over the entire temperature range of approximately 500 K. That would mean that, even in the temperature range above T_A the melt dynamics would still exhibit a highly cooperative nature, which is in agreement with the observation of a vanishing isotope effect in the PdNiCuP liquid, extending from the undercooled melt to well above the liquidus temperature [50] .

On the other hand, at even higher temperatures, a further question remains as to whether the collectivity of the dynamics would decrease to such an extent that we would observe purely single-particle motion. This has been found, for example, in simulations of Zr-Cu alloys where, well above the liquidus temperature, the diffusion coefficient was able to be described by the SER as the loosely packed state is approached at high temperatures [15]. We compare here the $Ni_{66.7}B_{33.3}$ and $Ge_{66.7}Ni_{33.3}$ melts at temperatures where both Ni self-diffusion coefficients equal 3×10^{-9} $m^2\,s^{-1}$. This temperature corresponds to 1740 K for $Ni_{66.7}B_{33.3}$ and 1100 K for $Ge_{66.7}Ni_{33.3}$. For $Ni_{66.7}B_{33.3}$ this temperature still belongs to the regime where we observe $D\eta \approx$ const.

Therefore, it seems that, as long as the presence of collective dynamics is concerned, the packing fraction is the more important factor, as $Ni_{66.7}B_{33.3}$ at 1740 K still exhibits a considerably higher packing than $Ge_{66.7}Ni_{33.3}$ (for $Ni_{66.7}B_{33.3}$ $\phi \approx 0.5$; for $Ge_{66.7}Ni_{33.3}$ $\phi \approx 0.43$), rather than the absolute scale of the melt dynamics.

IV. CONCLUSION

Through the techniques of ESL, high-temperature rheometry, and QENS, we were able to obtain accurate experimental data for density, viscosity, and self-diffusion of $Ni_{66.7}B_{33.3}$ and $Ge_{66.7}Ni_{33.3}$ melts. The measurements enabled investigation of the relationship between viscous flow and atomic self-diffusion in both densely and loosely packed metallic melts. The loosely packed $Ge_{66.7}Ni_{33.3}$ liquid alloy ($\phi < 0.5$) shows the temperature-dependent trend predicted by the SER. In contrast, the densely packed liquid alloy $Ni_{66.7}B_{33.3}$ shows $D\eta =$ const, in contradiction to the SER ($D\eta \propto T$) but in line with a similar densely packed alloy, $Zr_{64}Ni_{36}$ [12]. In the case of $Ge_{66.7}Ni_{33.3}$, we attribute this behavior to the lower packing fraction of the liquid alloy, whereas, for $Ni_{66.7}B_{33.3}$, the relatively high packing fraction necessitates the collective movement of multiple atomic particles diffusing through the liquid, thus leading to the observed breakdown in the SER.

ACKNOWLEDGMENTS

We would like to thank B. Nowak, S. Szabo, and D. Holland-Moritz for their help during the experiment at the research neutron source Heinz Maier-Leibnitz (FRM II). Furthermore, we thank J. Brillo and A. J. Rawson for a critical reading of the manuscript.

[1] A. Einstein, *Investigations on the Theory of Brownian Movement* (Dover, New York, 1926).
[2] J.-P. Hansen and I. R. McDonald, *Theory of Simple Liquids: With Applications to Soft Matter* (Academic, London, 2013).
[3] W. Sutherland, London, Edinburgh Dublin Philos. Mag. J. Sci. **9**, 781 (1905).
[4] H. R. Schober and H. L. Peng, Phys. Rev. E **93**, 052607 (2016).
[5] J. P. Poirier, Geophys. J. Int. **92**, 99 (1988).
[6] G. Clough, J. Physiol. **328**, 389 (1982).
[7] H. J. Parkhurst and J. Jonas, J. Chem. Phys. **63**, 2698 (1975).
[8] H. J. Parkhurst and J. Jonas, J. Chem. Phys. **63**, 2705 (1975).
[9] J. Jonas and J. A. Akai, J. Chem. Phys. **66**, 4946 (1977).
[10] K. Binder and W. Kob, *Glassy Materials and Disordered Solids: An Introduction to Their Statistical Mechanics* (World Scientific, Singapore, 2011).
[11] A. Bartsch, K. Rätzke, A. Meyer, and F. Faupel, Phys. Rev. Lett. **104**, 195901 (2010).
[12] J. Brillo, A. I. Pommrich, and A. Meyer, Phys. Rev. Lett. **107**, 165902 (2011).
[13] A. Meyer, W. Petry, M. Koza, and M.-P. Macht, Appl. Phys. Lett. **83**, 3894 (2003).
[14] S. K. Das, J. Horbach, and T. Voigtmann, Phys. Rev. B **78**, 064208 (2008).
[15] X. J. Han and H. R. Schober, Phys. Rev. B **83**, 224201 (2011).
[16] X. J. Han, J. G. Li, and H. R. Schober, J. Chem. Phys. **144**, 124505 (2016).
[17] F. Affouard, M. Descamps, L.-C. Valdes, J. Habasaki, P. Bordat, and K. L. Ngai, J. Chem. Phys. **131**, 104510 (2009).
[18] P. Bordat, F. Affouard, M. Descamps, and F. Müller-Plathe, J. Phys.: Condens. Matter **15**, 5397 (2003).
[19] W. Kob and H. C. Andersen, Phys. Rev. E **51**, 4626 (1995).
[20] S. K. Kumar, G. Szamel, and J. F. Douglas, J. Chem. Phys. **124**, 214501 (2006).
[21] S. R. Becker, P. H. Poole, and F. W. Starr, Phys. Rev. Lett. **97**, 055901 (2006).
[22] J. Horbach and W. Kob, Phys. Rev. B **60**, 3169 (1999).
[23] A. Jaiswal, T. Egami, and Y. Zhang, Phys. Rev. B **91**, 134204 (2015).
[24] S. W. Basuki, F. Yang, E. Gill, K. Rätzke, A. Meyer, and F. Faupel, Phys. Rev. B **95**, 024301 (2017).
[25] W. Götze and L. Sjögren, Rep. Prog. Phys. **55**, 241 (1992).
[26] H. R. Schober, Physics **4**, 80 (2011).
[27] T. Iwashita, D. M. Nicholson, and T. Egami, Phys. Rev. Lett. **110**, 205504 (2013).
[28] Q.-L. Cao, P.-P. Wang, and D.-H. Huang, Phys. Chem. Chem. Phys. **22**, 2557 (2020).
[29] M. Blodgett, T. Egami, Z. Nussinov, and K. Kelton, Sci. Rep. **5**, 13837 (2015).

[30] W. K. Rhim, S. K. Chung, D. Barber, K. F. Man, G. Gutt, A. Rulison, and R. E. Spjut, Rev. Sci. Instrum. **64**, 2961 (1993).
[31] T. Kordel, D. Holland-Moritz, F. Yang, J. Peters, T. Unruh, T. Hansen, and A. Meyer, Phys. Rev. B **83**, 104205 (2011).
[32] I. Jonas, W. Hembree, F. Yang, R. Busch, and A. Meyer, Appl. Phys. Lett. **112**, 171902 (2018).
[33] P. Heintzmann, F. Yang, S. Schneider, G. Lohöfer, and A. Meyer, Appl. Phys. Lett. **108**, 241908 (2016).
[34] H. Lamb, Proc. London Math. Soc. **s1–13**, 51 (1881).
[35] M. Kehr, W. Hoyer, and I. Egry, Int. J. Thermophys. **28**, 1017 (2007).
[36] D. Ferris and P. N. Quested, NPL Report CMMT (A) 306, NPL London (2002).
[37] R. Roscoe, Proc. Phys. Soc. London **72**, 576 (1958).
[38] A. Meyer, S. Stüber, D. Holland-Moritz, O. Heinen, and T. Unruh, Phys. Rev. B **77**, 092201 (2008).
[39] D. Holland-Moritz, S. Stber, H. Hartmann, T. Unruh, and A. Meyer, J. Phys.: Conf. Ser. **144**, 012119 (2009).
[40] T. Unruh, J. Neuhaus, and W. Petry, Nucl. Instrum. Methods Phys. Res., Sect. A **580**, 1414 (2007).
[41] A. J. Dianoux, G. H. Lander, and I. Laue-Langevin, *Neutron Data Booklet* (Old City Publishing, 628 North Second Street, Philadelphia, PA 19123 USA, 2003).
[42] FRIDA, http://apps.jcns.fz juelich.de/doku/frida/.
[43] L. Pauling, J. Am. Chem. Soc. **69**, 542 (1947).
[44] E. A. Brandes and G. B. Brook, *Smithells Metals Reference Book*, 7th ed. (Butterworths/Heinemann, London, United Kingdom, 1992).
[45] T. Halm, W. Hoyer, H. Neumann, and R. Bellissent, Z. Naturforsch. A **48**, 452 (1993).
[46] S. Nell, F. Yang, D. Holland-Moritz, Th. Voigtmann, J. Hu, T. Buslaps, T. Hansen, and A. Meyer (unpublished).
[47] T. Ishikawa, P.-F. Paradis, N. Koike, and Y. Watanabe, Rev. Sci. Instrum. **80**, 013906 (2009).
[48] W. Götze, *Complex Dynamics of Glass-Forming Liquids: A Mode-Coupling Theory*, Vol. 143 (Oxford University Press, New York, 2008).
[49] F. Yang, T. Unruh, and A. Meyer, Europhys. Lett. **107**, 26001 (2014).
[50] V. Zöllmer, K. Rätzke, F. Faupel, and A. Meyer, Phys. Rev. Lett. **90**, 195502 (2003).